ACS APPLIED MATERIALS & INTERFACES

Letter

www.acsami.org

Nanoimprinting Sub-100 nm Features in a Photovoltaic Nanocomposite using Durable Bulk Metallic Glass Molds

Jonathan P. Singer,[†,‡] Manesh Gopinadhan,[†,‡] Zhen Shao,[†,§] André D. Taylor,[†] Jan Schroers,[§] and Chinedum O. Osuji*[,†]

[†]Department of Chemical and Environmental Engineering and [§]Department of Mechanical Engineering and Materials Science, Yale University, New Haven, Connecticut 06511, United States

Supporting Information

ABSTRACT: The use of bulk metallic glass (BMG) for the nanoimprint of high-aspect-ratio (>3) features into functional polymers is investigated. To accomplish this, the most critical aspect is the successful demolding of the imprinted polymer. By fluorosilane functionalization of the BMG surface and optimization of processing temperature, high aspect pore features down to 45 nm diameters are introduced into the surface of two organic photovoltaic systems: poly(3-hexylthiophene-2,5-diyl) (P3HT) and 1:1 mixtures of P3HT with Phenyl-C61-butyric acid methyl ester (PCBM). The crystallinity of P3HT demands higher forming temperatures and pressures that are difficult to obtain with conventional soft nanoimprint lithography molds. The ability to accommodate a wide range of processing conditions and the low cost of fabricating molds with nanometer-scale features point to the large potential of nanotextured BMGs as an economical and scalable imprint material for high-resolution applications.

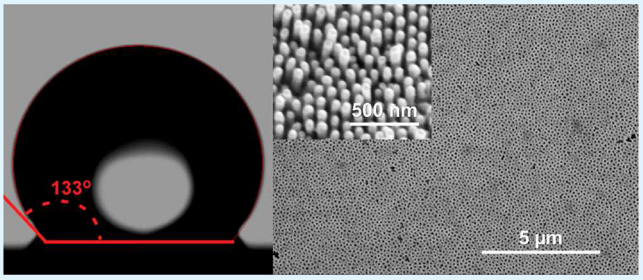

KEYWORDS: *nanoimprint lithography, bulk metallic glass, polymer patterning, organic photovoltaics, bulk heterojunctions*

Bulk metallic glasses (BMGs) are metastable amorphous metals that lack any intrinsic nanoscale crystalline structure. As a consequence, they exhibit superb mechanical properties such as very high strength, elasticity, hardness, shear resistance, and toughness. These mechanical properties are often paired with a unique processing opportunity, which is based on the characteristic that they undergo a continuous transition in viscosity between their solid and liquid state.[1,2] Because of this, alloys optimized for suppressed crystallization can be processed in a highly viscous supercooled liquid state analogous to the thermoplastic forming utilized for polymer manufacturing.[3] For this reason, BMG materials are effective for the inverted replication of hard templates by hot embossing above their glass transition temperature.[4,5] Additionally, BMG patterns have been themselves used as nanoimprint lithography (NIL) masters by the transfer of these replicated features to similarly softenable materials.[4] As NIL materials, BMGs' ability to both act as a moldable material and an imprint master place them in comparison to both typical hard die materials (e.g., silicon) and also soft replica-forming materials (e.g., polydimethylsiloxane (PDMS)).

Compared to hard dies, BMGs possess the advantages of high durability and elasticity that prevents the catastrophic brittle failure that can occur in silicon which limits the reuse of silicon masters. At the same time, BMG molds allow for smooth, nanostructured features whose ultimate maximum resolution is not limited by the presence of grains. Replication of atomic-level smoothness has been demonstrated[6] and these capabilities continue to be investigated. In comparison to soft replica materials, BMGs can be formed in a more rapid fashion, can support high-resolution structures with large aspect ratios due to their rigidity ($E \approx$ 100 GPa) and strength and toughness that are enhanced at small sizes,[7] and some can be completely recycled by melting and recasting. Further, the stiffness of BMGs allows for imprint to be done at high pressure, such as is required for, for example, thermal NIL below the relevant softening (i.e., melting/glass transition) temperature of the target material. On the basis of these comparisons, another way to consider the unique traits BMGs is that they possesses materials properties that allow it to both be an effective master and NIL material (see the Supporting Information).

Despite the impressive potential for BMG-based NIL, there have been surprisingly few studies to date regarding nanoimprint of functional materials. These have further been focused primarily on poly(methyl methacrylate) as a generic example of a thermoplastic material.[4,8−11] In particular, imprint in the regime of sub-100 nm features (d) and aspect ratios (h/d) >1−2 have not been thoroughly explored. This is a regime of great interest to functional and mesoscale polymer (e.g., block copolymer) systems. As one example, these length scales are relevant for polymer and organic photovoltaic applications.

Ordered bulk heterojunction (OBHJ) structures formed of semiconducting organic materials are one potential area where

Received: October 24, 2014
Accepted: January 31, 2015
Published: January 31, 2015

DOI: 10.1021/am507368g
ACS Appl. Mater. Interfaces 2015, 7, 3456−3461

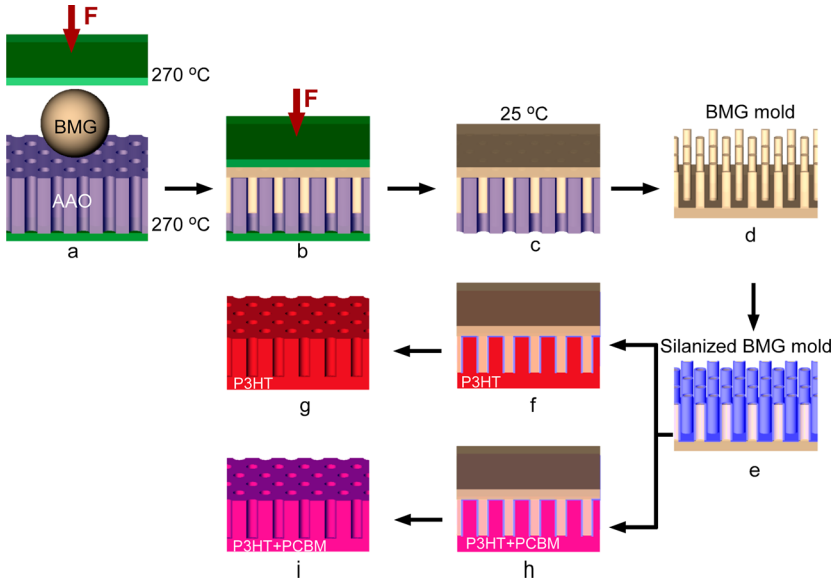

Figure 1. Schematic of the nanomolding of (a–d) Pt-BMG and (e–i) NIL processes on organic photovoltaics using the BMG master.(a) Pt-BMG bead placed on AAO molds was heated to 270 °C, above the glass transition temperature (T_g = 235 °C), but below the crystallization temperature (T_x = 305 °C). b) BMG was extruded into the AAO cavities at a final loading of >5kN for 3 min at a constant loading rate. (c) The sample was then cooled to room temperature and (d) BMG master was released by etching AAO template in NaOH aqueous solution (20 wt %) at 70 °C for 6h. (e) The BMG mold was then silanized to facilitate demolding. Two distinct geometries of organic photovoltaics were fabricated by BMG imprint. (f, g) Thin film nanoimprinting in (f) P3HT and (h) P3HT:PCBM blends. Imprinting was performed at 160 °C and the BMG master was released at room temperature. (h, i): Imprinting onto P3HT:P3BM 1:1 was performed at 140 °C, and the mold release at room temperature results in P3HT:PCBM nanostructured materials.

the ability to imprint nanostructures is highly desirable. Recent efforts have demonstrated that the use of NIL results in beneficial alignment of P3HT molecules,[12] whereas nanoconfinement of P3HT and PCBM donor/acceptor mixtures to nanoscale pores increases the performance of OBHJ and other organic semiconductor devices by enhanced mobility and phase separation[13] and also induces alignment of the P3HT in the blend[14] and enhanced optical trapping.[15] To this end, the NIL of organic systems for OBHJs has recently been demonstrated by several groups.[16−21] Ideal OBHJ sample geometries consist of domain sizes for the donor and acceptor phases commensurate to twice the exciton diffusion length (~20−30 nm) and thicknesses on the order of hundreds of nanometers.[22,23] These lateral dimensions are easily accessible to NIL, and 25 nm imprinted P3HT domains imprinted into PCBM leading to ~20% efficiency increase in an OBHJ.[16] These OBHJ structures, as well as the other demonstrations, have been so far limited in their maximum height, with aspect ratios of 3 or less. Extensions to high aspect ratio structures could enable for harvesting of a greater proportion of incident light as the device thickness approaches optical length scales while maintaining exciton-scale lateral dimensions, as was demonstrated in a recent simulation and meta-analysis study of OBHJ structures.[24]

As discussed, BMGs can serve as both imprint masters and imprint molds, but the limits of their capabilities for high-resolution and high-aspect ratio patterning has yet to be systematically explored. BMG replicas can be trivially transferred to PDMS by standard methods (Supporting Information), where contact energy is low and demolding is simplified by the soft deformation of the PDMS. The likely reason that this regime has not been approached in BMGs for thermal imprint is that surface functionalization has been relatively underutilized for BMG systems for lowering the demolding stress. In the case of noble metal BMG alloys, such as the Pt-BMG used here for its superior formability, the stability of such coatings is also an open question. This study therefore aims to demonstrate sub-100 nm, >3 aspect ratio structures imprinted into functional polymer systems at elevated temperatures enabled by surface functionalization. The goal is to prove the capabilities of BMGs to reach these features as, most importantly, a replica material, since such features are not achievable through PDMS molding. This therefore would place BMG materials as an attractive intermediate step for a more expensive, high-precision lithographic process to extend the lifetime of, for example, silicon masters.

To accomplish this, we highlight replication and demolding of high-aspect-ratio BMG structures into the active polymeric materials (here both of poly(3-hexylthiophene-2,5-diyl) (P3HT) and mixtures of P3HT with phenyl-C61-butyric acid methyl ester (PCBM)) with applications in OBHJ photovoltaic devices through the use of fluorosilane surface-functionalized BMG molds. In considering the potential for devices, BMG-based imprint can serve as a method to scalably fabricate OBHJ geometries in two distinct ways (illustrated in Figure 1): (1) a nanostructured electrode in a phase separated, nanoconfined OBHJ of P3HT and PCBM produced by imprint and (2) an OBHJ of P3HT and PCBM with conventional electrode performed by imprint into P3HT, removal of the template, and (not explored here) subsequent introduction of PCBM into the template by consecutive imprint into softened PCBM, such as has been performed previously for similar systems,[16,25] or spinning of PCBM out of an orthogonal solvent.

As a representative example of high aspect ratio templates, anodized aluminum oxide (AAO) templates (Synkera Technologies Inc.) were used to enable high-throughput testing of nanoscale features with sub-100 nm characteristic dimensions. These consist of nanoscale holes of various sizes on a disordered triangular lattice, and were used to generate arrays of BMG

DOI: 10.1021/am507368g
ACS Appl. Mater. Interfaces 2015, 7, 3456−3461

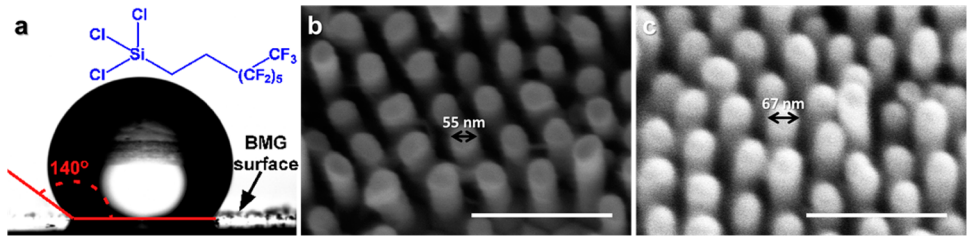

Figure 2. Surface energy of the BMG molds was tuned by coating with trichloro(1H,1H,2H,2H perfluoro-octyl)silane either from a solution phase or vapor phase. (a) Silane-functionalized BMG master surface behaved as hydrophobic with contact angle ~140°. Compared to (b) the as-prepared 55 nm BMG mold, after surface coating, (c) the size of the rods moderately increases while maintaining the shape because of the conformal nature of the vapor phase treatment. All scale bars are 300 nm.

nanopillars through the previously reported method as illustrated in Figure 1 (details in the Supporting Information).[4]

One of the most critical factors in using BMG for imprinting of active polymer systems is the ability to demold the BMG from the polymer after imprint. To first order, this problem may be considered as a competition between the relative surface energies of the polymer with the substrate and the BMG, which can be expressed as the following criterion for a template consisting of hexagonally packed cylinders, eq 1

$$1 > \frac{W_{M-P}SA_{M-P}}{W_{P-S}SA_{P-S}} = \frac{W_{M-P}}{W_{P-S}}\frac{\frac{\sqrt{3}a^2}{2} + \pi dh}{\frac{\sqrt{3}a^2}{2}}$$

$$\approx \left.\frac{2\pi dhW_{M-P}}{\sqrt{3}a^2W_{P-S}}\right|_{h\gg a} \quad (1)$$

where W is the indicated surface energy with M representing the metal, P representing the polymer, and S representing the substrate, SA the indicated surface area, d is the diameter of the pillar, h the height, and a is the spacing between cylinders. There are several important implications of this criterion. For example, although it is clearly more difficult to imprint higher-aspect-ratio structures, the parabolic dependence on lattice spacing can greatly reduce the effects of feature height. What is most important, however, is that, because $d > a$, the surface energy between the BMG and the polymer cannot exceed that of the polymer and the substrate for any aspect ratio >1. Although both of these parameters can be tuned, the polymer−substrate interface can be critical for device performance and therefore may not be freely selected. Because of this, the key parameter is the surface energy between the mold and polymer, which is quite high on freshly generated BMG molds even without texturing, as evidenced by detachment of the polymer films from silicon and glass upon pressing.

Surface treatment of the BMG to reduce the interfacial tension between the BMG and polymer was introduced as a means of mitigating the detachment issue highlighted above. This was done by silanization, as has been utilized in BMG functionalization in the past:[26] Samples were treated with plasma to introduce hydroxyl groups on the thin native oxide at the BMG surface. This was followed by chemical binding of a fluorinated silane to the BMG (details in the Supporting Information). The resulting surfaces displayed water contact angles exceeding 130° (Figure 2) in most cases, as compared to ~90° before treatment. The contact angles were largely insensitive to temperature up to 170 °C, which is above the maximum utilized NIL process temperature here of 160 °C for repeated imprints, though a small number of imprints could be successfully performed at higher temperatures. This thermal stability of the silane coating is important for the fidelity of the replication process and permits reuse of the mold multiple times before a new coating must be performed. The silane coating results in a slight change in diameter of the samples, in a typical example as shown in Figure 2b, c, where a silane layer thickness of 6−10 nm is observed under SEM. Detailed description of the surface functionalization is given in the Supporting Information.

We explored the ability to imprint the functionalized BMG structures with various nanorod sizes and spacings into both the P3HT and P3HT:PCBM 50:50 mixed system with a home-built apparatus that allowed us to heat the films to 160 and 140 °C, respectively, well above the glass transition temperatures of both materials (<100 °C) and below the melting temperatures (200−220 °C).[27] One current necessity is that the films be made thicker (2−5 μm) than ideal devices (100−300 nm) to account for macroscopic variations in the flatness of the mask and our limited ability to align the mask and sample. Both of these issues are previously solved engineering challenges that will require more complex apparatus, but present no fundamental problem with the processing. For example, thin-film patterning is possible over smaller areas (200−500 μm, see the Supporting Information, Figure S3), but because of the limitations in uniformity with our current system, results in damage to both the polymer and BMG. Figure 3 shows representative images of untreated masks, imprints, and resultant cross-sections successfully produced in P3HT and P3HT:PCBM for the smallest feature sizes explored (manufacturer's specification of average pore size of 35 and 55 nm, translating to treated feature sizes of ~45 and ~65 nm, respectively). These features transferred in millimeter scale patterns (see the Supporting Information, Figure S4), limited by contact area and the size of the patterned regions of the discs. The BMG molds produced from the 35 nm AAO displayed incomplete rod coverage due to features in the AAO, thus resulting in similar incomplete coverage in the imprinted films. The best results were obtained with imprints into the P3HT:PCBM blend due to the relative softness of this phase by the melting point depression, repeatedly showing transferred aspect ratios of ~4. From the standpoint of OPV, aspect ratios on this scale are ideal as they allow for features with sizes commensurate to the exciton length with thicknesses commensurate to optical wavelengths and extinction lengths. The molds could be reused multiple times (tested to up to 12 times) without loss in the fidelity of the patterning (Figure 4a−c) or the coating (see Supporting Information, Figure S5).

Patterning flexibility and durability is of critical importance. We also explored the ability to tune the processing conditions to obtain denser patterns or facilitate molding and detachment to further the capabilities for patterning. Patterns that were dense (i.e., $a/d \approx 2$) in the sub-100 nm regime could not be patterned successfully at high-aspect ratio (Supporting Information, Figure S7)

DOI: 10.1021/am507368g
ACS Appl. Mater. Interfaces 2015, 7, 3456−3461

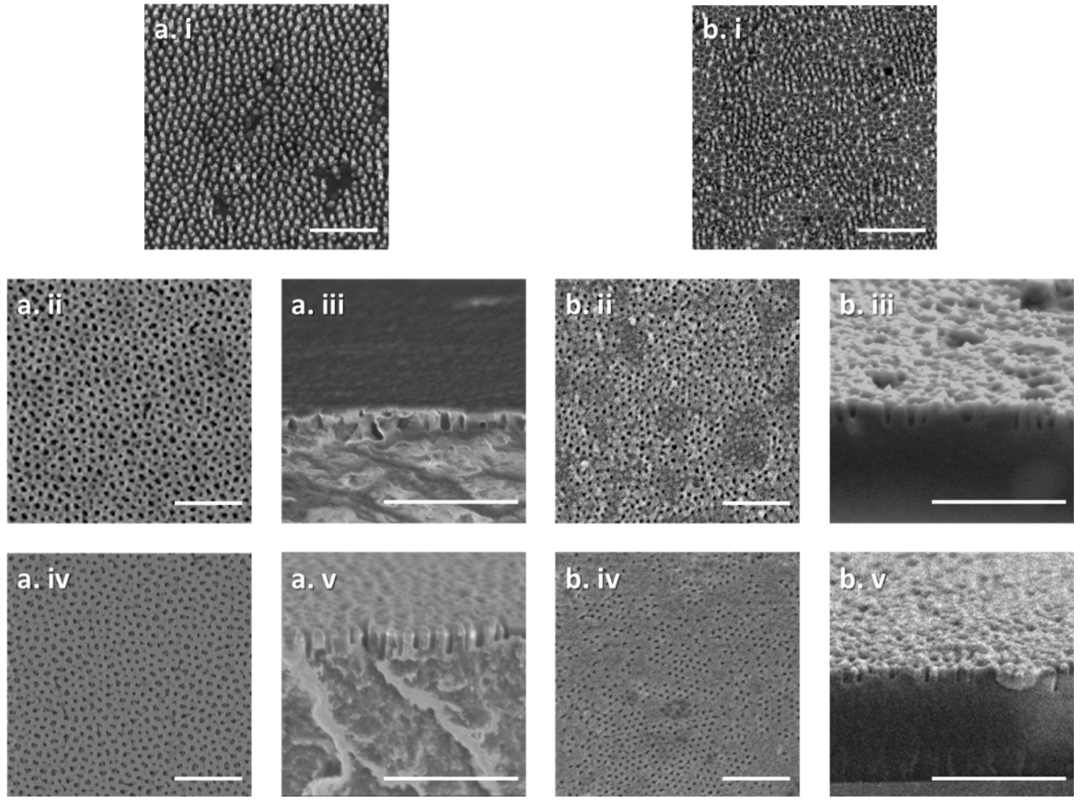

Figure 3. (a) 55 and (b) 35 nm BMG templates (i) viewed at an angle of 25° along with (ii, iv) resulting imprints and (iii, v) 75° cross-sections of resulting imprints in (ii, iii) P3HT and (iv, v) P3HT:PCBM demonstrating imprint aspect ratios of up to four. All scale bars are 1 μm.

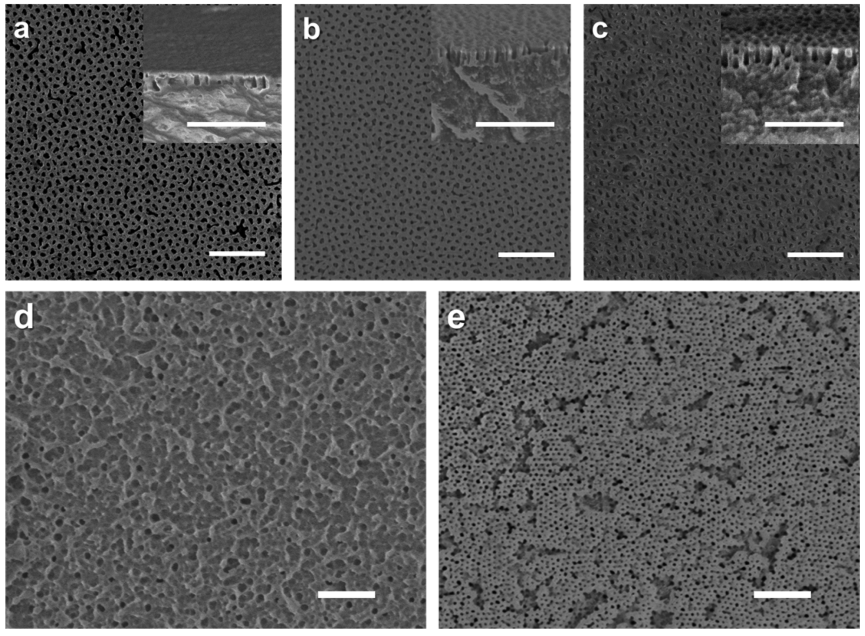

Figure 4. (a–c) Multiple imprint from the same BMG 55 nm pattern into the different polymer systems along with cross-sections in inset: (a) first imprint into P3HT, (b) fourth imprint into P3HT:PCBM, and (c) seventh imprint into a poly(styrene-*b*-dimethylsiloxane) block copolymer (performed at 180 °C). (d, e) P3HT:PCBM films damaged through suboptimal imprint temperatures: (d) detachment of the film due to imprint stress at 180 °C and (e) uneven advancement of the imprint front at 120 °C. All scale bars are 1 μm.

due to the implications of eq 1. An additional consideration not represented by eq 1 is the importance of thermal expansion to the detachment process. This can be a useful effect as the organic material (possessing a larger thermal expansion coefficient than the BMG) would be expected to contract to a larger extent upon cooling, leading to strains at the interface that should aid in detachment. If this change in volume is too large, however, the wires may be "gripped" by the shrinking polymer leading to fracturing and pull-off of the material, as has been studied previously from a purely mechanical standpoint.[28] To avoid the

DOI: 10.1021/am507368g
ACS Appl. Mater. Interfaces 2015, 7, 3456–3461

discontinuous jump in volume that occurs upon recrystallization, imprint temperatures below the melting point of the crystalline polymer systems were utilized. At the same time, the temperature had to be high enough to decrease the viscosity of the polymer enough to prevent uneven viscous advance of the imprint front. Images of imprints performed at these suboptimal regimes are shown in Figure 4d, e.

We have demonstrated the imprint and demolding of P3HT and P3HT:PCBM mixtures using surface-functionalized BMG molds possessing feature sizes down to ∼45 nm and resultant structure aspect ratios of up to and exceeding 3 over a large area. The most important implication of these results is that the BMG template utilized to perform this imprint could be reused multiple times (7 imprints shown without loss of patterning fidelity, however some masks used 10−12 times without coating loss) before the functionalization lost its effectiveness. Even at this point, patterning could be potentially continued by cleaning and refunctionalizing the surface as mechanical damage to the sample is not expected in these highly elastic, durable materials (e.g., BMG rods were not observed to be embedded into the sample during any experiments). This is in stark contrast to silicon or photoresist masters which are brittle and undergo plastic deformation respectively, which would suggest a patterning route of generating highly deliberate BMG masters through replication of a conventional silicon structure. When considered as a replica (rather than master) material in comparison to PDMS, the BMG replicas demonstrate here flexibility in both their thermal range and mechanical robustness. In the latter case, we were able to perform high-aspect-ratio forming of crystalline materials at temperatures below melting, which in this case is an essential regime for successful detachment of the resultant patterns without either uneven front formation (temperature too low) or thermal expansion-induced gripping (temperature too high). In the latter regard, the maximum imprint temperature explored was 180 °C; however, the alloy employed here can remain a glass for extended periods of processing time (several hours) up to 200 °C,[29] and higher glass transition (∼305 °C vs 235 °C) Pd-based alloys have demonstrated similar high-aspect-ratio formability.[30]

In short, these experiments show the potential of BMGs, possessing both desirable features as master and replica medium, as a low cost, durable material for the nanopatterning of functional materials. Specifically, demolding, the main challenge in nanoimprint in general, can be readily achieved by a combination of a lowered surface energy, optimized processing temperature, and the superb mold properties of BMGs. What is necessary for furthering the application of BMGs to NIL is scaling of both the replication molding process for nanostructured samples, heretofore limited to sub-centimeter scale, and the NIL process. As one example, issues with uniformity of the mold and replicas could be addressed by using larger, more uniform initial masters, such that a more uniform central imprinted region could be generated with less variation in pillar height. Further, both of these issues can be greatly aided through the application of the precision currently utilized in commercial soft NIL apparatus to the higher viscosity forming of BMGs to generate flat, uniform BMG molds, and the precedent of such innovations is greatly encouraging for the prospect of advancing this method to device-scale demonstrations.

■ ASSOCIATED CONTENT

Ⓢ Supporting Information

Experimental conditions for silanization, schematic of BMG capabilities, AFM of PDMS replica of 35 nm sample, data on temperature stability of silanization, low-magnification SEM image of 55 nm P3HT sample, SEM images of patterns from dense BMG rods, and image of stability of silanization after multiple imprints. This material is available free of charge via the Internet at http://pubs.acs.org.

■ AUTHOR INFORMATION

Corresponding Author

*E-mail: chinedum.osuji@yale.edu. Phone: (203) 432-4347.

Author Contributions

‡The manuscript was written through contributions of all authors. All authors have given approval to the final version of the manuscript. J.P.S. and M.G. contributed equally.

Funding

This work was supported by NSF through DMR-1119826 and ONR YIP award N000141210657. Facilities use was supported by YINQE and DMR-1119826. C.O.O. and J.P.S. acknowledge support from a Dubinsky New Initiative Award.

Notes

The authors declare no competing financial interest.

■ ACKNOWLEDGMENTS

The authors thank Dr. Su Huang, Candice I. Pelligra, and Brittany Rauzan for conducting preliminary studies; Dr. Sungwoo Sohn and Punnathat Bordeenithikasem for assistance in BMG alloy casting; and Dr. Ze Liu, Dr. Yanhui Liu, and Professor Judy Cha for useful discussions in the development of this work.

■ REFERENCES

(1) Ashby, M. F.; Greer, A. L. Metallic Glasses as Structural Materials. *Scr. Mater.* **2006**, *54* (3), 321−326.

(2) Schroers, J. Bulk Metallic Glasses. *Phys. Today* **2013**, *66* (2), 32−37.

(3) Schroers, J.; Paton, N. Amorphous Metal Alloys Form like Plastics. *Adv. Mater. Processes* **2006**, *164* (1), 61−63.

(4) Kumar, G.; Tang, H. X.; Schroers, J. Nanomoulding with Amorphous Metals. *Nature* **2009**, *457* (7231), 868−872.

(5) Sharma, P.; Kaushik, N.; Kimura, H.; Saotome, Y.; Inoue, A. Nano-Fabrication with Metallic Glass—An Exotic Material for Nano-Electromechanical Systems. *Nanotechnology* **2007**, *18* (3), 035302.

(6) Kumar, G.; Staffier, P. A.; Blawzdziewicz, J.; Schwarz, U. D.; Schroers, J. Atomically Smooth Surfaces through Thermoplastic Forming of Metallic Glass. *Appl. Phys. Lett.* **2010**, *97* (10), 101907.

(7) Kumar, G.; Desai, A.; Schroers, J. Bulk Metallic Glass: The Smaller the Better. *Adv. Mater.* **2011**, *23* (4), 461−476.

(8) Chen, Y. C.; Chu, J. P.; Jang, J. S. C.; Hsieh, C. W.; Yang, Y.; Li, C. L.; Chen, Y. M.; Jeng, J. Y. Replication of Nano/Micro-Scale Features using Bulk Metallic Glass Mold Prepared by Femtosecond Laser and Imprint Processes. *J. Micromech. Microeng.* **2013**, *23* (3), 035030.

(9) Zhang, N.; Chu, J. S.; Byrne, C. J.; Browne, D. J.; Gilchrist, M. D. Replication of Micro/Nano-Scale Features by Micro Injection Molding with a Bulk Metallic Glass Mold Insert. *J. Micromech. Microeng.* **2012**, *22* (6), 065019.

(10) Pan, C. T.; Wu, T. T.; Chen, M. F.; Chang, Y. C.; Lee, C. J.; Huang, J. C. Hot Embossing of Micro-Lens Array on Bulk Metallic Glass. *Sens. Actuators A* **2008**, *141* (2), 422−431.

(11) Chu, J. P.; Wijaya, H.; Wu, C. W.; Tsai, T. R.; Wei, C. S.; Nieh, T. G.; Wadsworth, J. Nanoimprint of Gratings on a Bulk Metallic Glass. *Appl. Phys. Lett.* **2007**, *90* (3), 034101.

(12) Hlaing, H.; Lu, X.; Hofmann, T.; Yager, K. G.; Black, C. T.; Ocko, B. M. Nanoimprint-Induced Molecular Orientation in Semiconducting Polymer Nanostructures. *ACS Nano* **2011**, *5* (9), 7532−7538.

(13) Allen, J. E.; Yager, K. G.; Hlaing, H.; Nam, C.-Y.; Ocko, B. M.; Black, C. T. Implementing Nanometer-Scale Confinement in Organic

DOI: 10.1021/am507368g
ACS Appl. Mater. Interfaces 2015, 7, 3456−3461

Semiconductor Bulk Heterojunction Solar Cells. *J. Photonics Energy* **2012**, *2* (1), 021008−1−021008−9.
(14) Johnston, D. E.; Yager, K. G.; Hlaing, H.; Lu, X.; Ocko, B. M.; Black, C. T. Nanostructured Surfaces Frustrate Polymer Semiconductor Molecular Orientation. *ACS Nano* **2014**, *8* (1), 243−9.
(15) Ko, D.-H.; Tumbleston, J. R.; Gadisa, A.; Aryal, M.; Liu, Y.; Lopez, R.; Samulski, E. T. Light-Trapping Nano-Structures in Organic Photovoltaic Cells. *J. Mater. Chem.* **2011**, *21* (41), 16293−16303.
(16) He, X.; Gao, F.; Tu, G.; Hasko, D. G.; Hüttner, S.; Greenham, N. C.; Steiner, U.; Friend, R. H.; Huck, W. T. S. Formation of Well-Ordered Heterojunctions in Polymer:PCBM Photovoltaic Devices. *Adv. Funct. Mater.* **2011**, *21* (1), 139−146.
(17) Yang, Y.; Mielczarek, K.; Aryal, M.; Zakhidov, A.; Hu, W. Nanoimprinted Polymer Solar Cell. *ACS Nano* **2012**, *6* (4), 2877−2892.
(18) Chen, D.; Zhao, W.; Russell, T. P. P3HT Nanopillars for Organic Photovoltaic Devices Nanoimprinted by AAO Templates. *ACS Nano* **2012**, *6* (2), 1479−1485.
(19) Tomohiro, K.; Hoto, N.; Kawata, H.; Hirai, Y. Fine Pattern Transfer of Functional Organic Polymers by Nanoimprint. *J. Photopolym. Sci. Technol.* **2011**, *24* (1), 71−75.
(20) Park, J. Y.; Hendricks, N. R.; Carter, K. R. Solvent-Assisted Soft Nanoimprint Lithography for Structured Bilayer Heterojunction Organic Solar Cells. *Langmuir* **2011**, *27* (17), 11251−11258.
(21) Choi, D.-G.; Lee, K.-J.; Jeong, J.-H.; Hwan Wang, D.; Ok Park, O.; Hyeok Park, J. Sub-100 nm Scale Polymer Transfer Printing Process for Organic Photovoltaic Devices. *Sol. Energy Mater. Sol. Cells* **2013**, *109*, 1−7.
(22) Weickert, J.; Dunbar, R. B.; Hesse, H. C.; Wiedemann, W.; Schmidt-Mende, L. Nanostructured Organic and Hybrid Solar Cells. *Adv. Mater.* **2011**, *23* (16), 1810−1828.
(23) Lee, Y.-H.; Lee, Y.-P.; Chiang, C.-J.; Shen, C.; Chen, Y.-H.; Wang, L.; Dai, C.-A. In Situ Fabrication of Poly (3-hexylthiophene)/ZnO Hybrid Nanowires with D/A Parallel-Lane Structure and Their Application in Photovoltaic Devices. *Macromolecules* **2014**, *47* (16), 5551−5557.
(24) Kim, J.; Kim, K.; Hwan Ko, S.; Kim, W. Optimum design of ordered bulk heterojunction organic photovoltaics. *Sol. Energy Mater. Sol. Cells* **2011**, *95* (11), 3021−3024.
(25) He, X.; Gao, F.; Tu, G.; Hasko, D.; Hüttner, S.; Steiner, U.; Greenham, N. C.; Friend, R. H.; Huck, W. T. S. Formation of Nanopatterned Polymer Blends in Photovoltaic Devices. *Nano Lett.* **2010**, *10* (4), 1302−1307.
(26) Liu, K.; Li, Z.; Wang, W.; Jiang, L. Facile Creation of Bio-Inspired Superhydrophobic Ce-Based Metallic glass Surfaces. *Appl. Phys. Lett.* **2011**, *99* (26), 261905.
(27) Ngo, T. T.; Nguyen, D. N.; Nguyen, V. T. Glass Transition of PCBM, P3HT and Their Blends in Quenched State. *Adv. Nat. Sci.: Nanosci. Nanotechnol.* **2012**, *3* (4), 045001.
(28) Hirai, Y.; Yoshida, S.; Takagi, N. Defect Analysis in Thermal Nanoimprint Lithography. *J. Vac. Sci. Technol., B* **2003**, *21* (6), 2765−2770.
(29) Legg, B. A.; Schroers, J.; Busch, R. Thermodynamics, Kinetics, and Crystallization of Pt57.3Cu14.6Ni5.3P22.8 Bulk Metallic Glass. *Acta Mater.* **2007**, *55* (3), 1109−1116.
(30) Arora, H. S.; Xu, Q.; Xia, Z.; Ho, Y.-H.; Dahotre, N. B.; Schroers, J.; Mukherjee, S. Wettability of Nanotextured Metallic Glass Surfaces. *Scr. Mater.* **2013**, *69* (10), 732−735.

DOI: 10.1021/am507368g
ACS Appl. Mater. Interfaces 2015, 7, 3456−3461